Dynamic Remodeling of Microbial Biofilms by Functionally Distinct Exopolysaccharides

Su Chuen Chew, Binu Kundukad, Thomas Seviour, et al.
2014. Dynamic Remodeling of Microbial Biofilms by Functionally Distinct Exopolysaccharides . mBio 5(4): . doi:10.1128/mBio.01536-14.

RESEARCH ARTICLE

Dynamic Remodeling of Microbial Biofilms by Functionally Distinct Exopolysaccharides

Su Chuen Chew,[a,b] Binu Kundukad,[d] Thomas Seviour,[b] Johan R. C. van der Maarel,[d,e] Liang Yang,[b,c] Scott A. Rice,[b,c,f] Patrick Doyle,[d,g] Staffan Kjelleberg[b,c,f]

Interdisciplinary Graduate School[a] and Singapore Centre on Environmental Life Sciences Engineering,[b] School of Biological Sciences,[c] Nanyang Technological University, Singapore; BioSystems and Micromechanics IRG, Singapore-MIT Alliance for Research and Technology[d] and Department of Physics,[e] National University of Singapore, Singapore; Centre for Marine Bio-Innovation and School of Biotechnology and Biomolecular Science, University of New South Wales, Sydney, NSW, Australia[f]; Department of Chemical Engineering, Massachusetts Institute of Technology, Cambridge, Massachusetts, USA[g]

ABSTRACT **Biofilms are densely populated communities of microbial cells protected and held together by a matrix of extracellular polymeric substances. The structure and rheological properties of the matrix at the microscale influence the retention and transport of molecules and cells in the biofilm, thereby dictating population and community behavior. Despite its importance, quantitative descriptions of the matrix microstructure and microrheology are limited. Here, particle-tracking microrheology in combination with genetic approaches was used to spatially and temporally study the rheological contributions of the major exopolysaccharides Pel and Psl in *Pseudomonas aeruginosa* biofilms. Psl increased the elasticity and effective cross-linking within the matrix, which strengthened its scaffold and appeared to facilitate the formation of microcolonies. Conversely, Pel reduced effective cross-linking within the matrix. Without Psl, the matrix becomes more viscous, which facilitates biofilm spreading. The wild-type biofilm decreased in effective cross-linking over time, which would be advantageous for the spreading and colonization of new surfaces. This suggests that there are regulatory mechanisms to control production of the exopolysaccharides that serve to remodel the matrix of developing biofilms. The exopolysaccharides were also found to have profound effects on the spatial organization and integration of *P. aeruginosa* in a mixed-species biofilm model of *P. aeruginosa-Staphylococcus aureus*. Pel was required for close association of the two species in mixed-species microcolonies. In contrast, Psl was important for *P. aeruginosa* to form single-species biofilms on top of *S. aureus* biofilms. Our results demonstrate that Pel and Psl have distinct physical properties and functional roles during biofilm formation.**

IMPORTANCE **Most bacteria grow as biofilms in the environment or in association with eukaryotic hosts. Removal of biofilms that form on surfaces is a challenge in clinical and industrial settings. One of the defining features of a biofilm is its extracellular matrix. The matrix has a heterogeneous structure and is formed from a secretion of various biopolymers, including proteins, extracellular DNA, and polysaccharides. It is generally known to interact with biofilm cells, thus affecting cell physiology and cell-cell communication. Despite the fact that the matrix may comprise up to 90% of the biofilm dry weight, how the matrix properties affect biofilm structure, maturation, and interspecies interactions remain largely unexplored. This study reveals that bacteria can use specific extracellular polymers to modulate the physical properties of their microenvironment. This in turn impacts biofilm structure, differentiation, and interspecies interactions.**

Received 2 July 2014 **Accepted** 7 July 2014 **Published** 5 August 2014

Citation Chew SC, Kundukad B, Seviour T, van der Maarel JRC, Yang L, Rice SA, Doyle P, Kjelleberg S. 2014. Dynamic remodeling of microbial biofilms by functionally distinct exopolysaccharides. mBio 5(4):e01536-14. doi:10.1128/mBio.01536-14.

Editor Rita Colwell, University of Maryland

Address correspondence to Staffan Kjelleberg, LASKJELLEBERG@ntu.edu.sg.

This article is a direct contribution from a Fellow of the American Academy of Microbiology.

Bacteria form surface-attached biofilm communities in nature and are significant in the context of environmental sustainability and health care (1, 2). Integral to the biofilm is a matrix of extracellular polymeric substances (EPS). The EPS form a heterogeneous viscoelastic material that holds the microbial cells together and account for 50 to 90% of the total organic matter in the biofilm (3). Division of labor in metabolism, gene transfer, and quorum sensing are facilitated in the biofilm because the matrix is responsible for maintaining the spatial organization of cells in the biofilm (4, 5).

The EPS are largely composed of polysaccharides, proteins, nucleic acids, humic acids, and lipids and determine the architecture of the biofilm (6). For example, biofilms assume many, often highly differentiated forms during development, including mushroom-like microcolonies and filamentous streamers, as well as a homogenous, undifferentiated layer of cells. The physical properties of the matrix determine the shape and mechanical stability of biofilms (7, 8) and affect processes such as mass transfer and detachment kinetics of the various differentiated forms. For example, EPS shearing can form sieve-like networks that result in rapid accumulation of cells and other dispersed biomass that results in the formation of biofilm streamers (9). Sloughing and

TABLE 1 Characteristics of the strains used in this study

Phenotype	Genotype	Description
Alg$^+$ Pel$^+$ Psl$^+$	Δ*mucA*	Overexpresses alginate, wild type
Alg$^+$ Pel$^-$ Psl$^+$	Δ*mucA* Δ*pelA*	Overexpresses alginate, no Pel
Alg$^+$ Pel$^+$ Psl$^-$	Δ*mucA* Δ*pslBCD*	Overexpresses alginate, no Psl
Alg$^+$ Pel$^-$ Psl$^-$	Δ*mucA* Δ*pelA* Δ*pslBCD*	Overexpresses alginate, no Pel and Psl
Alg$^-$ Pel$^+$ Psl$^+$	PAO1	Minimal or no alginate, wild type
Alg$^-$ Pel$^-$ Psl$^+$	Δ*pelA*	Minimal or no alginate, no Pel
Alg$^-$ Pel$^+$ Psl$^-$	Δ*pslBCD*	Minimal or no alginate, no Psl

dispersal via the detachment of streamer tails from biofilms depend on the mechanical failure of the EPS (8). The EPS matrix also responds to the chemical composition of the environment, where osmotic pressure gradients have been shown to be responsible for the surface spreading of biofilms (10). Finally, the physical response of biofilms to flow has been shown to have an impact on community composition and succession (11). Despite many such observations of its importance, quantitative descriptions of the physical properties of the matrix and its impact on biofilm architecture and composition are limited.

Pseudomonas aeruginosa is an opportunistic pathogen that causes a wide range of hospital-acquired infections (12). *P. aeruginosa* has also been found to coexist with *Staphylococcus aureus* in the lungs of cystic fibrosis patients and in chronic wounds (13, 14). *P. aeruginosa* is known to produce three different exopolysaccharides that can potentially be components of the biofilm matrix. Alginate, which consists mainly of mannuronic and guluronic acid residues, is often overexpressed in *P. aeruginosa* strains isolated from chronically infected cystic fibrosis patients (15). Alginate overexpression protects *P. aeruginosa* from host immune responses and antibiotics (16) and gives the biofilm a mucoid phenotype. However, alginate was shown not to be essential for biofilm structure maintenance (17). Psl and Pel have been found to play important roles in biofilm formation (18, 19). Psl and Pel have overlapping structural roles, and deletions of both genes in the laboratory strain PAO1 significantly impair biofilm formation (20, 21). The structures of Psl and Pel have yet to be fully elucidated, but carbohydrate analyses indicate that Psl is mannose and galactose rich and Pel is glucose rich (18, 19). Studies have indicated that Psl can wrap itself around *P. aeruginosa* cells to thus contribute to cell surface attachment and microcolony formation (22, 23). However, the contribution of Pel to the biofilm life cycle in *P. aeruginosa* strains that contain both the *pel* and *psl* operons remains unclear.

Particle-tracking microrheology is an optical technique that measures the rheological properties by tracking the Brownian motion of spherical probes or particles within the sample (24, 25). The mean squared displacement (MSD), $\langle \Delta r^2(t) \rangle$, of the particles undergoing Brownian motion over time, t, is related to the mechanical properties of the substance in which the particles are suspended according to $\langle \Delta r^2(t) \rangle \alpha t^{\alpha}$ where $\alpha = 1$ for viscous fluids, $0 < \alpha < 1$ for viscoelastic substances, and $\alpha = 0$ for elastic substances. Viscous fluids show irreversible deformation to stress, whereas elastic materials return to their original shape after the removal of stress. The MSD is directly proportional to and can be used to calculate the creep compliance of the material, which is the tendency of the material to deform permanently over time. Low MSD values and high elasticity are a consequence of high degrees of polymeric cross-linking (i.e., effective cross-linking) (26, 27). Such cross-linking can be chemical through covalent bonds, or physical from noncovalent interactions, such as ionic and hydrogen bonds (28, 29) and topological constraints from entanglements of polymer chains (30).

Previous microrheological experiments have mapped the mechanical properties of biofilms according to the height and location within the flow cell (31, 32). However, the difference in rheological properties of specific biofilm structures, such as the microcolonies or undifferentiated regions, was not investigated. Furthermore, a direct link between the molecular components of the matrix and local biofilm rheology and function has not yet been established. In this study, particle-tracking microrheology, in combination with confocal laser scanning microscopy, was used to characterize the local viscoelasticities of *P. aeruginosa* biofilms at different stages of development. The contributions of Pel and Psl exopolysaccharides to biofilm rheology during development were investigated in *P. aeruginosa* strains with the clinically relevant mucoid phenotype that expresses the combination of the three exopolysaccharides (Alg$^+$ Pel$^+$ Psl$^+$) and mutant derivatives (Alg$^+$ Pel$^+$ Psl$^-$, Alg$^+$ Pel$^-$ Psl$^+$, and Alg$^+$ Pel$^-$ Psl$^-$) (33). To assess the rheological roles of Pel and Psl in the absence of alginate, nonmucoid *P. aeruginosa* strains expressing a combination of Pel and Psl exopolysaccarides (Alg$^-$ Pel$^+$ Psl$^+$, Alg$^-$ Pel$^-$ Psl$^+$, and Alg$^-$ Pel$^+$ Psl$^-$) (20) were also investigated (Table 1). This allowed the rheological impact of exopolysaccharides to the biofilm in the context of population and community behavior to be explored using single-species *P. aeruginosa* streamer as well as *P. aeruginosa*-*S. aureus* mixed-species biofilm assays.

RESULTS

Particle distribution and size selectivity of biofilms. Mucoid *P. aeruginosa* biofilm cells expressing various combinations of the Psl and Pel exopolysaccharides were grown in a flow cell biofilm system for 5 days using medium containing 1.0-, 0.5-, and 0.2-μm fluorescent carboxylate-modified latex particles. The carboxylate modification reduced particle aggregation and binding to negatively charged cell surfaces (Invitrogen, CA). Alg$^+$ Pel$^+$ Psl$^+$ and Alg$^+$ Pel$^-$ Psl$^+$ cells formed similar biofilms with thin plains (the undifferentiated sections) and large microcolonies, (Fig. 1A and B). Alg$^+$ Pel$^+$ Psl$^-$ biofilms were less differentiated and delayed in development, forming thick plains and small microcolonies at the later stages (Fig. 1C). The Alg$^+$ Pel$^-$ Psl$^-$ cells were unable to form a biofilm on the coverslip (Fig. 1D). This is consistent with previous observations (34). Mucoid *P. aeruginosa* is known to revert back to its nonmucoid state after long periods of biofilm cultivation (35). To estimate the percentage of nonmucoid revertants in the strains, cells from 5-day biofilms were harvested and colony morphologies were observed. All colonies generated from the single and combination mutants retained their mucoid phenotypes,

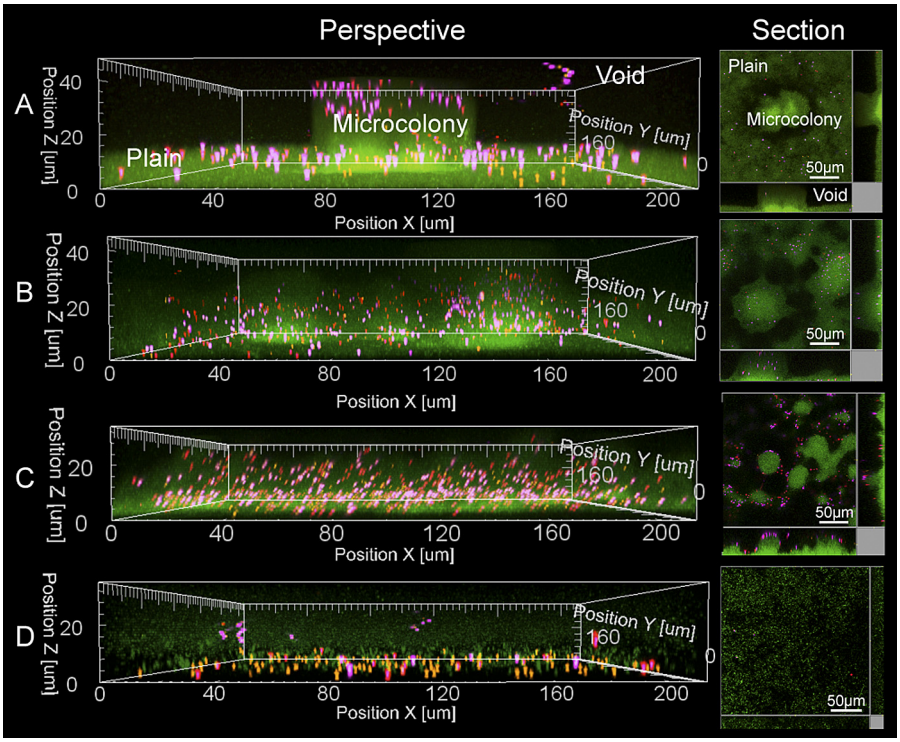

FIG 1 Perspective and sectional view of day 5 biofilms by confocal microscopy after continuous feeding with particles of sizes 1.0 (purple), 0.5 (red), and 0.2 (orange) μm upon inoculation of the flow cell. (A to C) Alg$^+$ Pel$^+$ Psl$^+$ (A), Alg$^+$ Pel$^-$ Psl$^+$ (B), and Alg$^+$ Pel$^+$ Psl$^-$ (C) biofilms. (D) Alg$^+$ Pel$^-$ Psl$^-$ cells attach poorly to the surface and do not form biofilm. Examples of microcolonies, plains, and voids are labeled in panel A.

indicating there was no change in the mucoid status of these strains under our experimental conditions (see Fig. S1 in the supplemental material).

Particles were incorporated from the medium into the three biofilm-forming strains (Alg$^+$ Pel$^+$ Psl$^+$, Alg$^+$ Pel$^-$ Psl$^+$, and Alg$^+$ Pel$^+$ Psl$^-$), with increased uptake of the larger particles relative to the smaller particles. Particles were counted in 4- and 5-day biofilms, and the ratio of 1.0- to 0.5- and 0.2-μm particles was used as a measure of size selectivity in the three biofilm-forming strains (Fig. 2A). The Alg$^+$ Pel$^+$ Psl$^+$ biofilm had 1.0- to 0.5- and 0.2-μm particle ratios of 2.02 $\pm$ 0.41 and 4.13 $\pm$ 1.24, respectively, while Alg$^+$ Pel$^-$ Psl$^+$ biofilm displayed ratios of 1.85 $\pm$ 0.55 and 4.81 $\pm$ 1.12, respectively. The Alg$^+$ Pel$^+$ Psl$^-$ biofilm, which was significantly impaired in biofilm development, had lower 1.0- to 0.5- and 0.2-μm particle ratios of 1.52 $\pm$ 0.31 and 2.44 $\pm$ 0.73, respectively. It was observed that the preference for 1.0-μm particles over the smaller particles was predominant in the microcolonies (Fig. 3). Hence strains that expressed the Psl polysaccharide and that formed more differentiated biofilms gave higher ratios of 1.0- to 0.5- and 0.2-μm particles.

To determine whether surface properties of the particles affected their uptake in the biofilm, the biofilm was grown together with 1.0-μm sulfate- and carboxylate-modified particles. The sulfate-modified particle is more hydrophobic than the carboxylate-modified particle due to the sulfate modification being shorter than the pendant carboxylate chains, thus exposing more of the hydrophobic aromatic rings of the latex particle (Invitrogen, CA). There were no significant differences between uptake of sulfate- and carboxylate-modified particles (Fig. 2B). Few particles were associated with the non-biofilm-forming Alg$^+$ Pel$^-$ Psl$^-$ strain. These were instead found attached to the coverslip.

The size-selective incorporation of particles, where larger particles had the greatest access to the interior of the microcolonies, suggests that particle entry is not simply due to penetration through the matrix. To study the mechanism of particle capture by the biofilm, particles were fed into 3-day biofilms rather than from the beginning of the experiment. Confocal images of the biofilms were captured on day 5. Particles were absent in areas where the biofilm had formed by day 3, such as the bottom layer of the biofilm and the centers of microcolonies. Instead, particles were present in the areas of recent biofilm growth, such as the surface, within the top layer of the biofilm, and the exterior of microcolonies (Fig. 3A). Thus, the particles were unable to penetrate regions of high-cell-density layers and microcolonies. They attached to the biofilm surface and were assimilated into the biofilm as they were overgrown and internalized, accumulating at the top layer of the biofilm and microcolony exterior.

Given that particles did not readily penetrate the biofilm, it is likely that the higher accumulation of 1.0-μm particles resulted from processes taking place during microcolony formation. This phase is characterized by continuous matrix production and upward growth of the biofilm as cells divide and migrate upwards from the plain to form the microcolony structure (36). It is possible that as this occurs, 1.0-μm particles at the biofilm surface migrate into the developing microcolony structure, while the 0.5- and 0.2-μm particles slip through the matrix and thus are not effectively retained by the growing biofilm structure.

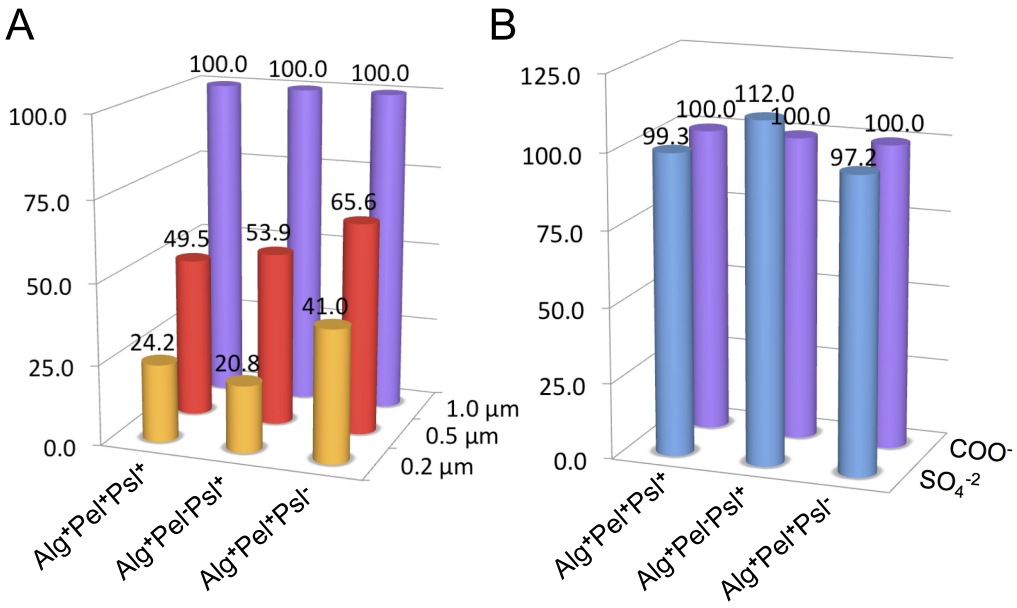

FIG 2 Ratios of various types of particles (*z* axis) in biofilm-forming strains (*x* axis) at days 4 and 5 after continuous feeding with particles upon inoculation of the flow cell. All particle numbers (*y* axis) are standardized to 100 particles of a size of 1.0 μm and carboxylate modification. (A) Ratio of carboxylate particles according to sizes of 1.0 (purple), 0.5 (red), and 0.2 (orange) μm. (B) Ratio of 1.0-μm particles according to carboxylate (purple) and sulfate (blue) surface modification.

Exopolysaccharide contributions to biofilm rheology. The viscoelastic properties of the biofilms formed by strains with different combinations of exopolysaccharides were explored by following the MSD and the creep compliance of the 1.0- and 0.5-μm particles embedded in different regions of the biofilms. These regions included the voids (medium above the biofilm), plains (flat layers of cells), and microcolonies (Fig. 1A). The MSD of the particles in the voids was comparable to the MSD of particles in pure medium, which was used as a control. In contrast, particles trapped in the biofilm vibrated at fixed positions, and the MSD values ranged from those typical of viscoelastic materials to those of strongly elastic gels (Fig. 4). The biofilms formed after 3 days of continuous flow culture, and the temporal changes in viscoelastic properties of the biofilm as the biofilm matured from days 3 to 5 were also determined.

Alg^+ Pel^+ Psl^+ cells formed microcolonies scattered on a thin plain on day 3. The MSD and creep compliance of the 1.0-μm particles in the microcolonies were independent of time and are characteristic of elastic behavior (Fig. 5A). The medians of the MSD and creep compliance (at $t = 1.5$ s) were on the order of 7.5×10^{-5} μm^2 and 4.3×10^{-4} Pa^{-1}, respectively, and indicate a higher effective cross-linking within 3-day microcolonies. By day 5, the microcolonies had developed into large distinct mushroom structures indicative of mature microcolonies. The MSD (4.3×10^{-4} μm^2) and creep compliance (2.8×10^{-3} Pa^{-1}) in these microcolonies increased, thus indicating a lower effective cross-linking within the matrix. The plain was too thin on day 3 to investigate its rheological properties without significant capillary effects from the substratum, and hence the microrheology of the plain was only determined on day 5. The microrheological profile

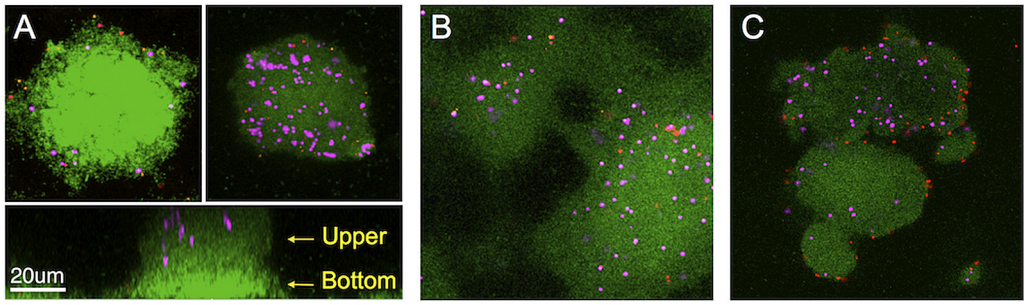

FIG 3 The number of 1.0-μm (purple) particles increases in the microcolonies over the smaller 0.5-μm (red) and 0.2-μm (orange) particles. Particles were placed into medium at day 3, and confocal images were captured at day 5. (A) Alg^+ Pel^+ Psl^+ microcolony. *xy* sections of the microcolony show that particles attach to the biofilm surface (top left) and are grown over, accumulating in newer areas of the biofilm, such as the upper part of the microcolony (top right). An *xz* section of the microcolony with the upper and bottom positions in the z-plane is shown below. (B and C) *xy* sections of the upper part of Alg^+ Pel^- Psl^+ (B) and Alg^+ Pel^+ Psl^- (C) microcolonies.

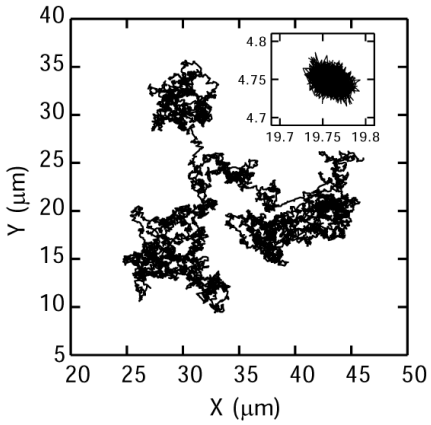

FIG 4 Trajectory of particles in the medium executing Brownian motion. The inset shows the trajectory of the particles in the microcolony.

of 5-day plains was close to that of 3-day microcolonies and could be reflective of their maturity.

The MSDs and corresponding creep compliance of 3-day microcolonies and 5-day plains in Alg$^+$ Pel$^-$ Psl$^+$ biofilms were similar to those of the Alg$^+$ Pel$^+$ Psl$^+$ strain, with median MSDs of 6.4 $\times$ 10^{-5} and 5.6 $\times$ 10^{-5} μm^2 and creep compliances of 3.6 $\times$ 10^{-4} and 3.2 $\times$ 10^{-4} Pa^{-1}, respectively (Fig. 5B). In contrast to Alg$^+$ Pel$^+$ Psl$^+$ biofilms, there was no change in the MSD as the microcolonies of Alg$^+$ Pel$^-$ Psl$^+$ cells matured. This suggests that Pel plays a role in the reducing the effective cross-linking within aging biofims. Despite the heterogenous morphology of the biofilms, the viscoelastic properties of the Alg$^+$ Pel$^-$ Psl$^+$ biofilms did not vary significantly throughout the biofilm.

Alg$^+$ Pel$^+$ Psl$^-$ cells formed the least differentiated biofilms of the strains tested, which largely consisted of thick plains that allowed for particle tracking on days 3 and 5. The MSD α t^{α} with exponent α less than 1 indicated that the biofilm had a viscoelastic behavior (Fig. 5C). The biofilm had median MSD and creep compliance values of 1.7 $\times$ 10^{-3} μm^2 and 1.1 $\times$ 10^{-2} Pa^{-1} on both days 3 and 5. Differentiation of the plains into microcolonies was only observed after day 3, and thus particle tracking could only be performed on 5-day microcolonies. The lowered MSD indicated that an increase in effective cross-linking in the matrix network is required for microcolony differentiation in Alg$^+$ Pel$^+$ Psl$^-$ biofilms. Thus, only the biofilms expressing both Pel and Psl exopolysaccharides displayed distinct rheological differences over time. Alg$^+$ Pel$^+$ Psl$^+$ and Alg$^+$ Pel$^-$ Psl$^+$ biofilms were initially similar in rheology, but as the Alg$^+$ Pel$^+$ Psl$^+$ biofilm matured, the most developed structures became less effectively cross-linked.

Alg$^+$ Pel$^-$ Psl$^-$ cells did not form biofilms and many were superficially attached to the substratum. It is suggested that the 1.0-μm particles were trapped in a thin extracellular material secreted by the cells. The graph of the MSD for the 1.0-μm particles exhibited a concave shape, indicating confined diffusion and that the particles were bound to a fixed point via an elastic link in the extracellular material (Fig. 5D).

The MSDs of the 0.5-μm particles in the microcolonies were lower than that of the 1.0-μm particles, indicating that they had had been captured by regions of greater effective cross-linking, reflective of their smaller size (Fig. 5E to G). Interestingly, the MSD of the 0.5-μm particles exhibited diffusive behavior at long time scales in 3-day microcolonies of Alg$^+$ Pel$^+$ Psl$^+$ and Alg$^+$ Pel$^-$ Psl$^+$ cells. It is possible that the smaller particles were able to move through the EPS mesh over a longer time scale. The reduced accumulation of 0.5- and 0.2-μm particles in the microcolonies indicates that they were unable to be retained into microcolonies, in contrast to the 1.0-μm particles. Thus, the matrix resembled a net that was able to capture and trap objects larger than its mesh size but did not capture objects similar to or smaller than its mesh size. In contrast to the 1.0-μm particles, the MSD of the 0.5-μm particles in 3-day microcolonies of Alg$^+$ Pel$^+$ Psl$^+$ cells did not increase by day 5 (Fig. 5A and E). However, the MSD of the 1-μm particles was more similar to the MSD of the 0.5-μm particles in the 5-day microcolonies of Alg$^+$ Pel$^+$ Psl$^-$ cells and supports the hypothesis that the contribution of Pel to the rheology of the microcolony increases over time (Fig. 5G). The 0.5-μm particles did not accumulate in the Alg$^+$ Pel$^-$ Psl$^-$ strain.

To examine whether the above effects of Pel and Psl were observable in their nonmucoid counterparts, microcolonies of Alg$^-$ Pel$^+$ Psl$^+$, Alg$^-$ Pel$^-$ Psl$^+$, and Alg$^-$ Pel$^+$ Psl$^-$ mutant strains were investigated (Fig. 5H). The nonmucoid strains were more effectively cross-linked than their mucoid counterparts. This could be due to a higher concentration of other matrix components, such as environmental DNA (eDNA) and pili, that has been observed in nonmucoid strains (37) or may be a direct rheological effect from the absence of alginate. It was found that the Alg$^-$ Pel$^-$ Psl$^+$ microcolonies had higher effective cross-linking than both Alg$^-$ Pel$^+$ Psl$^+$ and Alg$^-$ Pel$^+$ Psl$^-$ microcolonies. Like its mucoid counterpart, the Alg$^-$ Pel$^+$ Psl$^-$ strain also developed microcolonies later than the Alg$^-$ Pel$^+$ Psl$^+$ and Alg$^-$ Pel$^+$ Psl$^-$ strains. The 5-day Alg$^-$ Pel$^+$ Psl$^-$ microcolonies remained less effectively cross-linked than the 3-day microcolonies of the other strains. However, they were no longer as viscoelastic as their mucoid counterparts. The reduction in effective cross-linking of the Alg$^-$ Pel$^+$ Psl$^+$ microcolony was also observed from days 3 to 5. Thus, Psl contributes to a more elastic matrix with highly effective cross-linking, whereas Pel increases the malleability by loosening the matrix in both mucoid and nonmucoid *P. aeruginosa.*

Rheological differences affect streamer formation. Elastic materials reversibly deform under shear, whereas viscous materials irreversibly deform under shear. To test the hypothesis that Psl makes biofilms more elastic and thus resistant to deformation shear forces, whereas Pel makes the biofilm more malleable, a biofilm streamer cultivation system, which involved growing biofilms on a steel mesh, was developed to assess the correlation between the various *P. aeruginosa* EPS mutants and biofilm streamer morphology. During the cultivation of *P. aeruginosa* EPS mutant biofilms, Alg$^+$ Pel$^+$ Psl$^+$ cells initially formed rough surface-attached biofilms. In the later stages, the biofilms became smooth with enhanced spreading (Fig. 6A). Alg$^+$ Pel$^-$ Psl$^+$ cells formed rough surface-attached biofilms that developed tall microcolonies with minimal spreading (Fig. 6B). Alg$^+$ Pel$^+$ Psl$^-$ cells formed smooth biofilms with extensive streamer formation. In the later stages, the steel mesh was completely covered by the biofilms (Fig. 6C). Alg$^+$ Pel$^-$ Psl$^-$ cells attached to the mesh but could not form a biofilm (Fig. 6D).

Different roles of Pel and Psl for species integration within biofilm communities. To further explore the ecological impact of the rheological differences caused by Pel and Psl of *P. aeruginosa*, species integration within a dual-species biofilm comprised of *P. aeruginosa* and *Staphylococcus aureus* was investigated. Alg$^+$

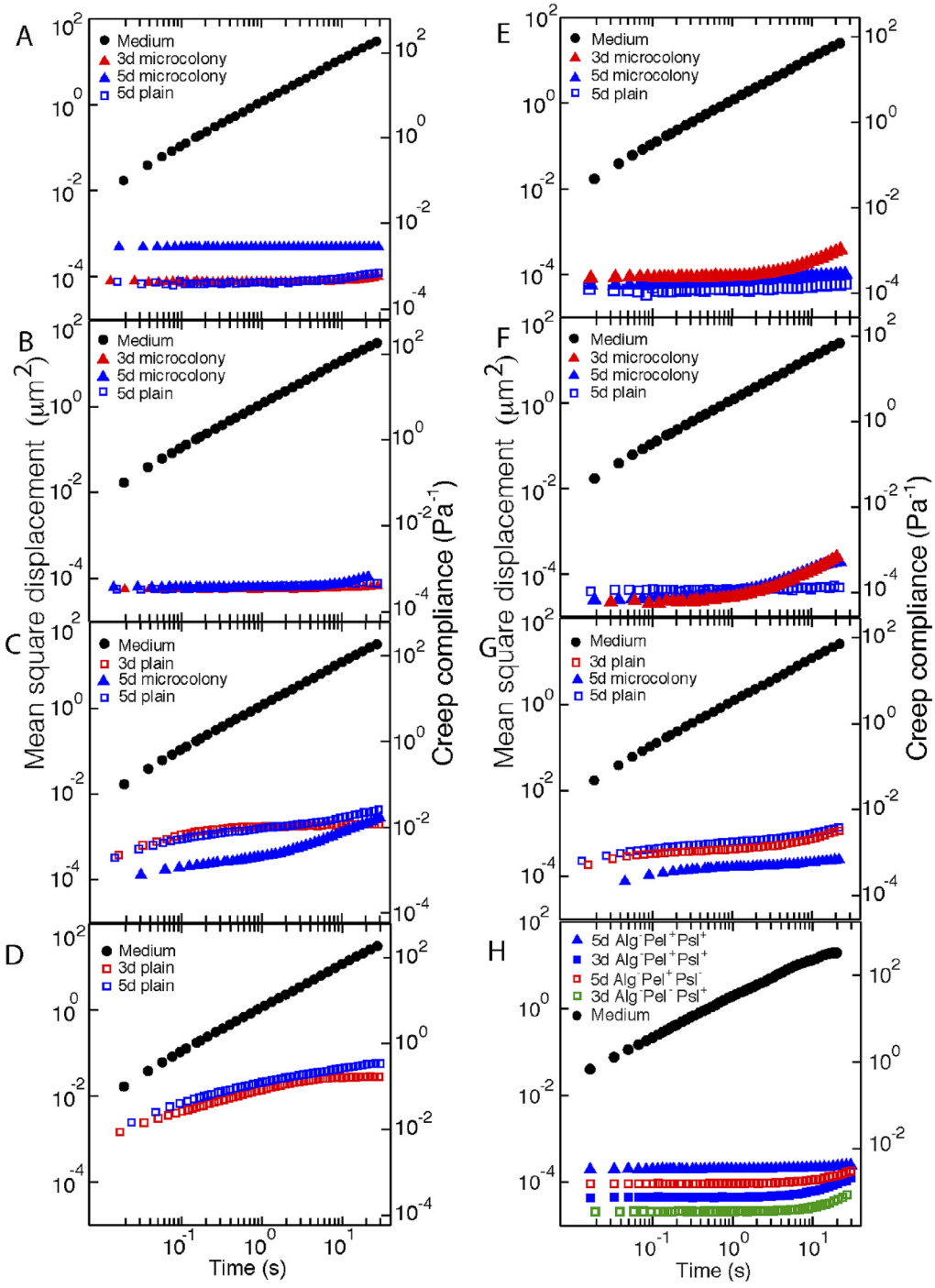

FIG 5 The left panels (A to D) show MSDs (left axis) and creep compliances (right axis) of 1.0-μm particles in biofilms expressing the Alg$^+$ Pel$^+$ Psl$^+$ strain (A), which is elastic and for which microcolonies are reduced in effective cross-linking from days 3 to 5, the Alg$^+$ Pel$^-$ Psl$^+$ strain (B), which is elastic and does not change in rheology from days 3 to 5, and the Alg$^+$ Pel$^+$ Psl$^-$ strain (C), which is viscoelastic and mainly consists of plains that do not change in rheology from days 3 to 5. (D) Biofilm is not formed in Alg$^+$ Pel$^-$ Psl$^-$ cells, and particle diffusion appears to be confined by extracellular secretion from a thin layer of cells. The right panels (E to H) show MSDs and creep compliances of 0.5-μm particles in biofilms expressing the strains shown. (E) The Alg$^+$ Pel$^+$ Psl$^+$ strain is elastic, and the diffusivity of particles increases at long time scales in 3-day microcolonies, indicating that the biofilm mesh size exceeds 0.5 μm. By day 5, mesh size reduces and rheology is similar to that in Alg$^+$ Pel$^+$ Psl$^-$ microcolonies. (F) The Alg$^+$ Pel$^-$ Psl$^+$ strain is elastic, and the diffusivity of particles increases at long time scales in 3- and 5-day microcolonies. The rheological properties of the microcolonies remain constant from days 3 to 5. (G) The Alg$^+$ Pel$^+$ Psl$^-$ strain is viscoelastic and mainly consists of plains that do not change in rheology from days 3 to 5. The 0.5-μm particles are not retained by the Alg$^+$ Pel$^-$ Psl$^-$ cell layer. The lower curves of 0.5-μm compared to 1.0-μm particles indicate that the smaller particles locate to regions of higher effective cross-linking. (H) MSDs of 1.0-μm particles in Alg$^-$ Pel$^+$ Pel$^+$, Alg$^-$ Pel$^-$ Psl$^+$, and Alg$^-$ Pel$^+$ Psl$^-$ microcolonies.

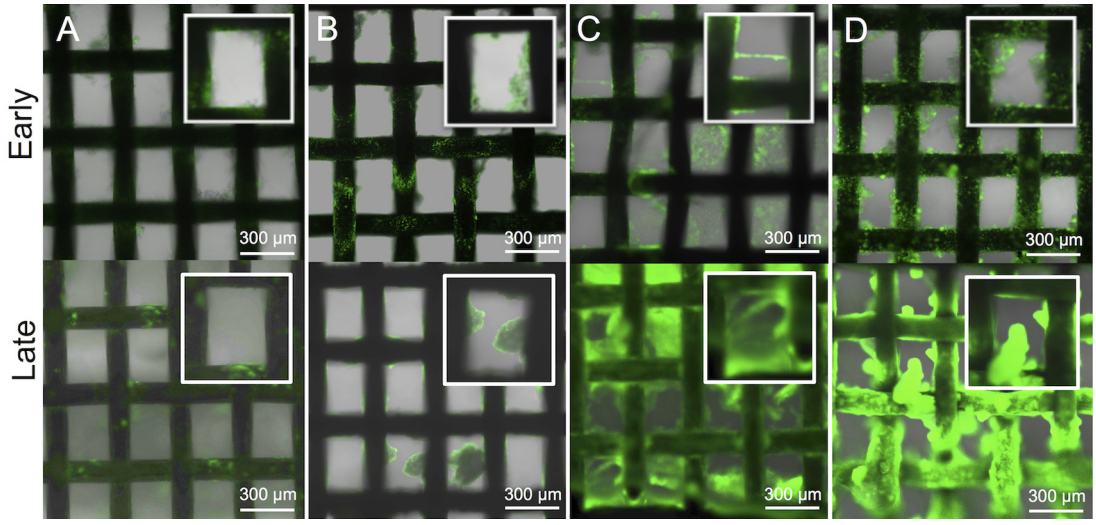

FIG 6 Confocal images of the various EPS mutants in the biofilm streamer cultivation system. Flow direction is horizontal (left to right) and parallel to the steel mesh. (A) Alg$^+$ Pel$^+$ Psl$^+$ cells initially forming rough surface-attached biofilms that become smooth with enhanced spreading. (B) Alg$^+$ Pel$^-$ Psl$^+$ cells forming rough surface-attached biofilms that develop large microcolonies with minimal spreading. (C) Alg$^+$ Pel$^+$ Psl$^-$ cells forming smooth biofilms with extensive streamer formation that extends across the mesh. (D) Alg$^+$ Pel$^-$ Psl$^-$ cells do not form biofilm. Insets show enlarged views of the biofilms.

Pel$^+$ Psl$^+$ *P. aeruginosa* cells and *S. aureus* formed biofilms comprised of two distinct layers. In the lower layer, *P. aeruginosa* and *S. aureus* were integrated into mixed-species microcolonies. In the upper layer, *P. aeruginosa* dominated the biofilm, forming monospecies biofilms that capped the microcolonies (Fig. 7A). Alg$^+$ Pel$^-$ Psl$^+$ *P. aeruginosa* cells did not associate with *S. aureus* and formed separate microcolonies at the substratum. *P. aeruginosa* also dominated the upper part of the biofilm, forming a monospecies biofilm layer on top of the microcolonies from both species (Fig. 7B). Alg$^+$ Pel$^+$ Psl$^-$ *P. aeruginosa* cells associated with *S. aureus* to form a mixed-species biofilm with a less prominent monospecies *P. aeruginosa* cap (Fig. 7C). Alg$^+$ Pel$^-$ Psl$^-$ *P. aeruginosa* cells were unable to associate with *S. aureus* and could only form small clusters of monospecies *P. aeruginosa* cells. The amount of *S. aureus* biofilm was minimal when grown in the presence of Alg$^+$ Pel$^-$ Psl$^-$ *P. aeruginosa* (Fig. 7D). Thus, Pel was required for integration of *P. aeruginosa* into mixed-species biofilms, while Psl promoted species segregation and monospecies biofilms. *P. aeruginosa* outcompeted *S. aureus* without the two polysaccharides.

DISCUSSION

Microrheological techniques can provide a more quantitative description of how different matrix components contribute to the

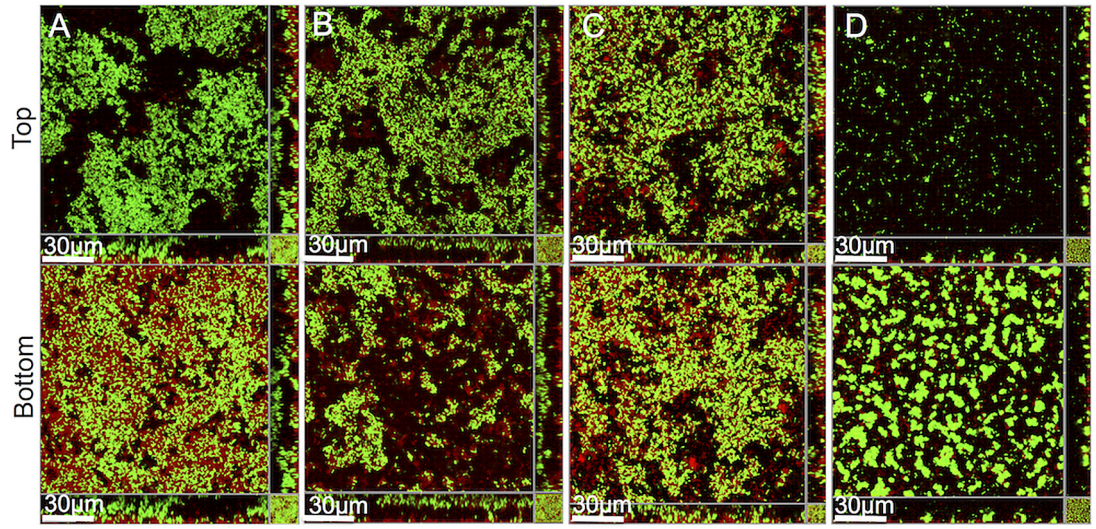

FIG 7 Polymicrobial biofilms of *Pseudomonas aeruginosa* (green) and *Staphylococcus aureus* (red). (A) Alg$^+$ Pel$^+$ Psl$^+$ *P. aeruginosa*-*S. aureus* mixed microcolonies at the substratum. Single-species *P. aeruginosa* biofilm caps the microcolonies. (B) Alg$^+$ Pel$^-$ Psl$^+$ *P. aeruginosa* does not mix with *S. aureus* at the substratum but forms single-species *P. aeruginosa* biofilm that also caps monospecies *S. aureus* microcolonies at the substratum. (C) Alg$^+$ Pel$^+$ Psl$^-$ *P. aeruginosa*-*S. aureus* mixed microcolonies with a reduced single-species *P. aeruginosa* biofilm cap. (D) Alg$^+$ Pel$^-$ Psl$^-$ *P. aeruginosa* forms small dense cell clusters with little spreading or microcolony formation.

rheology and function of biofilms. Specifically, particle-tracking microrheology was employed to study the contributions of Pel and Psl exopolysaccharides to the rheological properties of the biofilm matrix. We show here that that Psl favors the development of elastic biofilms with highly effective cross-linking, whereas Pel favors viscoelastic and loose biofilms. Biofilms expressing exclusively either Psl or Pel do not appear to change significantly in rheological properties over time. However, when both exopolysaccharides are produced, the biofilm becomes less effectively cross-linked within the mature parts of the biofilm, consistent with a shift in production of the dominant polysaccharides from Psl to Pel.

The reduction in effective cross-linking could be due to a reduction in the expression, release, or degradation of surface-bound Psl at the microcolony center prior to dispersal (22). While the generation of a Psl matrix-free cavity also probably occurs in Pel^{-} Psl^{+} strains, the absence of Psl could have resulted in a complete loss of biofilm and fast dispersal and expulsion of particles without Pel supporting the matrix. Thus, Psl contributes to a stiffer matrix during the initial stages of biofilm development, and Pel increases in contribution to and remodels the matrix into a more malleable structure at the later stages. *P. aeruginosa* is known to use multiple regulatory systems to control the synthesis of different EPS components during growth (4, 38), and the variation between Psl expression and Pel expression may represent an important adaptation strategy of *P. aeruginosa* in dynamic and fluctuating environments. We postulate that because young biofilms are thinner and less robust, a more cross-linked and elastic matrix that is relatively more resistant to external mechanical shear forces, such as brushing and rapid flows, is expressed. This would prevent cells from dispersing and thus centralize growth to the newly attached site when the biofilm has just been established and is less populated. After the biofilm has matured and is fully populated, Pel could be used to remodel the matrix to yield a more viscous biofilm. Unlike elastic materials that return to their original shape after stress is removed, viscous materials deform irreversibly when exposed to stress and hence can flow. Thus, a viscous biofilm can more effectively spread laterally to colonize new areas.

We have functionally validated the above hypothesis by growing the biofilm on a steel mesh to promote an alternative, bioprocess-relevant, biofilm morphology (i.e., that of streamers). Streamer formation is dependent on the malleability of the EPS of surface-attached biofilms and can cause rapid disruption of flow in industrial and medical systems (9). Biofilms expressing the Psl polysaccharide initially form a strongly surface-attached rough biofilm. When the Pel polysaccharide was also expressed, surface spreading of the biofilm was enhanced during maturation. Without the Pel polysaccharide, the biofilm spreads minimally and resists streamer formation. As the biofilm matures, it develops tall, rigid colonies. Expression of Pel in the absence of Psl polysaccharide results in extensive streamer formation that eventually fills the spaces between the mesh.

The rheological roles of Pel and Psl in regulating species integration within a dual-species biofilm model were also explored. In cocultures with *S. aureus*, Pel was required to form mixed-species biofilms with *S. aureus* at the substratum. Increased loosening and malleability of the *P. aeruginosa* matrix imparted by Pel may have allowed for *S. aureus* to infiltrate and associate with *P. aeruginosa* to produce an integrated, mixed-species biofilm. Alternatively,

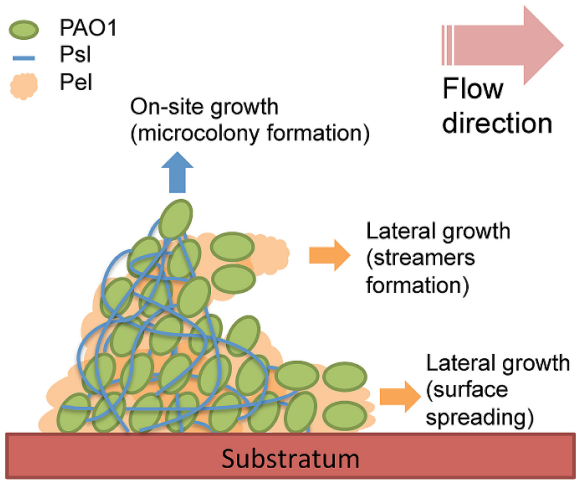

FIG 8 Schematic of *P. aeruginosa* streamer formation, in which Psl forms the surface-attached streamer head and Pel forms the streamer tail. Psl acts as stiff wires that build up the biofilm architecture and support on-site growth, such as the enlargement of microcolonies, whereas Pel acts as a spreader and filler important for expansion during the later stages of biofilm development.

the loosening of the matrix by Pel may have allowed for *P. aeruginosa* to interact and become incorporated with the *S. aureus* matrix (39). Psl expression favored species segregation and formed monospecies microcolonies of *P. aeruginosa* and *S. aureus*. The high effective cross-linking in the *P. aeruginosa* matrix conferred by Psl may have presented a physical barrier that did not allow for interaction with *S. aureus* strain. Without both polysaccharides, *P. aeruginosa* outcompeted the *S. aureus* in the form of tiny cell clusters spread across the substratum. Thus, the entrapment of *P. aeruginosa* into microcolonies by Psl appeared to provide more substratum space for *S. aureus* to colonize and establish a biofilm. Psl was also found to be important for dominance of monospecies *P. aeruginosa* biofilms at the upper layer of the biofilm and could result from Psl facilitating upward growth and microcolony expansion in *P. aeruginosa* biofilms.

We therefore suggest a new model for *P. aeruginosa* biofilm remodeling in which Psl is more elastic and acts as stiff wire-like structures to build the initial biofilm architecture and support on-site growth—e.g., the enlargement of existing microcolonies. Pel is more viscous and acts to allow spreading of cells in the matrix, which would be important for expansion during the later stages (Fig. 8). This complements previous studies that have shown that Psl is important for cell attachment (22), biofilm initiation, and microcolony development (20, 40), and Pel is important for pellicle formation (non-surface-attached or floating biofilm morphology) (19). The model presented here is based upon the early creep experiments conducted on *P. aeruginosa* streamers (8) and suggests that Psl is responsible for constructing the firmly surface-attached streamer head, while Pel designs the loose streamer tail. Recently, a combined optical and atomic force microscopy study has revealed that Psl expression results in cells tilting upwards off the surface, while Pel expression results in *P. aeruginosa* cells lying flat on surfaces (41). If cell orientation impacts the growth pattern, Psl would direct cells and growth upwards, increasing microcolony height, and Pel would direct cells to grow laterally for the spreading onto new surfaces, consistent with our model.

Regardless of the strain used, the microsized particles used do not penetrate the biofilm easily once formed. Instead, the particles are incorporated during the growth of the biofilm. Both particle-counting and passive microrheological experiments indicate that the biofilm exhibits a range of mesh sizes smaller than 1.0 μm. The 0.5-μm particles were apparently able to slip through the matrix in the microcolonies, indicating that the matrix mesh size is between 0.5 and 1.0 μm within the microcolonies. Drug delivery using particles to combat biofilms should also consider using particles larger than biofilm mesh size as these results indicate that they would assimilate more readily into the microcolonies than the smaller particles during biofilm growth.

In conclusion, particle-tracking microrheology can be used to spatially and temporally resolve the local mechanical properties of biofilms in real time at the microscale and are effective tools for studying biofilms. Our study shows how different parts of the biofilm can be remodeled using different components of the matrix and suggests that the production of Pel and that of Psl are differentially regulated during biofilm development. The flexibility of the matrix would be an important emergent property of the biofilm resulting from microbial adaption to growth conditions. This could have consequences for *P. aeruginosa* to compete or cooperate with coexisting species in the biofilm. The concept of modifying the physical properties of the biofilm by using natural components of the matrix has important implications for the guided engineering and control of biofilms for health care and industrial applications—for example, by expressing an elastic and highly cross-linked matrix to limit biofilm propagation by surface spreading and streamer formation or to resist invasion or incorporation of other microbial species.

MATERIALS AND METHODS

Bacterial strains. The *P. aeruginosa* Δ*mucA*, Δ*mucA* Δ*pelA*, Δ*mucA* Δ*pslBCD* and Δ*mucA* Δ*pelA* Δ*pslBCD* mucoid mutants are described in reference 33, and the *P. aeruginosa* wild-type strain PAO1 and the Δ*pelA* and Δ*pslBCD* mutants are described in reference 20. Fluorescence-tagged strains were constructed by the insertion of a mini-Tn*7*-enhanced green fluorescent protein (eGFP)-Gm^r cassette as described (42). Overnight cultures of *P. aeruginosa* strains were grown in Luria-Bertani broth (10 g liter^{-1} NaCl, 10 g liter^{-1} yeast extract, 10 g liter^{-1} tryptone), and overnight cultures of *S. aureus* 15981 strains (43) were grown in tryptic soy broth (TSB) (5 g liter^{-1} NaCl, 2.5 g liter^{-1} K_2HPO_4, 17 g liter^{-1} tryptone, 3 g liter^{-1} soytone, 0.25% [wt/vol] glucose) at 37°C under shaking conditions (200 rpm).

Cultivation of flow cell biofilms. Overnight *P. aeruginosa* cultures were diluted to an optical density at 600 nm (OD_{600}) of 0.4, and 350 μl was injected into the flow cell chambers with individual channel dimensions of 1 by 4 by 40 mm to grow biofilms. Biofilms were fed with 1× M9 medium (48 mM Na_2HPO_4, 22 mM KH_2PO_4, 19 mM NH_4Cl, 9 mM NaCl, 2 mM $MgSO_4$, 0.1 mM $CaCl_2$) supplemented with 0.04% (wt/vol) glucose and 0.2% (wt/vol) Casamino Acids at a flow rate of 5.5×10^{-3} m s^{-1} and room temperature of 25°C. The bacteria were initially allowed to attach to the coverslip substratum for 1 h before M9 medium was fed into the chambers using a Masterflex L/S 07523-80 peristaltic pump. For the development of biofilm streamers, a steel mesh of mesh size of 200 μm by 262.5 μm was fitted into the channels of the flow cell chamber. The flow system was assembled and prepared as described previously (44). Confocal images of the biofilms were taken on days 4 and 5 (Zeiss LSM780 confocal system).

Cultivation of static polymicrobial biofilms. Overnight cultures of mucoid *P. aeruginosa* and *S. aureus* cells were diluted 100-fold in TSB. The *P. aeruginosa* mucoid strains and mutants were each mixed 1:1 (vol/vol) with *S. aureus* to form the cocultures. μ-Slide 8-well microscopy chambers (ibidi, Munich, Germany) were inoculated with 200-μl concentrations of 1:1 (vol/vol) cocultures of mucoid *P. aeruginosa* and *S. aureus* and incubated for 1 day at 37°C under static conditions for biofilm formation. Biofilms were stained with SYTO62 (Invitrogen, CA) to allow visualization of *S. aureus*, and confocal images of the biofilms were taken on day 1 (Zeiss LSM780 confocal system).

Particle counting. Particles in the confocal images of biofilms captured at days 4 and 5 were counted using IMARIS software (Bitplane AG, Zurich, Switzerland). The particles were located using a Gaussian filter, and the initial thresholds were checked for accuracy. The size selectivity ratios for each strain are a mean of ratios calculated from a set of four confocal images, each covering a surface area of 212.55 μm by 212.55 μm. Errors are given as standard errors of the means.

Passive microrheology. Fluorescent particles (Invitrogen, CA) with diameters of 1.0, 0.5, and 0.2 μm were dispersed in the M9 medium to final concentrations of 2.18×10^6 particles ml^{-1} and continuously fed to the biofilm. This allowed for incorporation of the particles into the matrix during the course of biofilm development. The Brownian motion of the particles, driven by thermal energies (k_BT) was followed using fluorescence microscopy (Zeiss Axio Imager M1) on days 3 and 5. By monitoring the particle's mean squared displacement (MSD) over time, t, the viscoelastic properties of the biofilm can be measured. The MSD of the bead is proportional to the creep compliance, $J(t)$, of the material in which the bead is embedded according to the relation

$$J(t) = \frac{3\pi a}{2k_BT}\langle \Delta r^2(t) \rangle$$

where J is creep compliance, a is particle diameter, k_B is the Boltzman constant, and T is temperature. The exposure time is short enough to minimize dynamic error and the static error in the MSD as estimated by monitoring 1.0-μm immobilized beads. It is assumed that the structures of the biofilm that give rise to the viscoelastic properties are much smaller than the size of the beads. These measurements can be used to map out the spatial variations in biofilm's mechanics and microstructure. The particle trajectories were obtained with public domain tracking software http://physics.georgetown.edu/matlab/, and further analysis was performed using home-written MatLab scripts (30, 45). The MatLab scripts calculate the mean square displacement in two dimensions by averaging the widths of the distributions obtained in the x and y directions. Each MSD curve was calculated from a range of 5 to 10 videos of 1 to 2.5 min and a frame rate of approximately 30 to 75 frames per s.

SUPPLEMENTAL MATERIAL

Supplemental material for this article may be found at http://mbio.asm.org/lookup/suppl/doi:10.1128/mBio.01536-14/-/DCSupplemental.

Figure S1, TIF file, 1.4 MB.

ACKNOWLEDGMENTS

We acknowledge financial support from the Singapore Centre on Environmental Life Sciences Engineering (SCELSE), whose research is supported by the National Research Foundation Singapore, Ministry of Education, Nanyang Technological University and National University of Singapore, under its Research Centre of Excellence Program. We also acknowledge Singapore MIT Alliance for Research and Technology's research program in BioSystems and Micromechanics, whose research is supported by the National Research Foundation Singapore.

The authors declare they have no competing financial interests.

S.C, T.S., L.Y., S.R., and S.K. designed the experiments. S.C. and B.K. carried out the experiments. S.C., B.K., L.Y., S.R., P.D., and S.K. analyzed the data. L.Y., B.K., and J.M. provided experimental tools. S.C., L.Y., S.R., and S.K. wrote the manuscript.

REFERENCES

1. **Costerton JW, Lewandowski Z, Caldwell DE, Korber DR, Lappin-Scott HM.** 1995. Microbial biofilms. Annu. Rev. Microbiol. **49:**711–745. http://dx.doi.org/10.1146/annurev.mi.49.100195.003431.

2. **Hall-Stoodley L, Costerton JW, Stoodley P.** 2004. Bacterial biofilms: from the natural environment to infectious diseases. Nat. Rev. Microbiol. **2:**95–108. http://dx.doi.org/10.1038/nrmicro821.
3. **Flemming HC, Neu TR, Wozniak DJ.** 2007. The EPS matrix: the "house of biofilm cells." J. Bacteriol. **189:**7945–7947. http://dx.doi.org/10.1128/JB.00858-07.
4. **Harmsen M, Yang L, Pamp SJ, Tolker-Nielsen T.** 2010. An update on *Pseudomonas aeruginosa* biofilm formation, tolerance, and dispersal. FEMS Immunol. Med. Microbiol. **59:**253–268. http://dx.doi.org/10.1111/j.1574-695X.2010.00690.x.
5. **Fuqua WC, Winans SC, Greenberg EP.** 1994. Quorum sensing in bacteria: the LuxR-LuxI family of cell density-responsive transcriptional regulators. J. Bacteriol. **176:**269–275.
6. **Flemming HC, Wingender J.** 2010. The biofilm matrix. Nat. Rev. Microbiol. **8:**623–633. http://dx.doi.org/10.1038/nrmicro2415.
7. **Seviour T, Pijuan M, Nicholson T, Keller J, Yuan Z.** 2009. Gel-forming exopolysaccharides explain basic differences between structures of aerobic sludge granules and floccular sludges. Water Res. **43:**4469–4478. http://dx.doi.org/10.1016/j.watres.2009.07.018.
8. **Stoodley P, Lewandowski Z, Boyle JD, Lappin-Scott HM.** 1999. Structural deformation of bacterial biofilms caused by short-term fluctuations in fluid shear: an in situ investigation of biofilm rheology. Biotechnol. Bioeng. **65:**83–92. http://dx.doi.org/10.1002/(SICI)1097-0290(19991005)65:1<83::AID-BIT10>3.0.CO;2-B.
9. **Drescher K, Shen Y, Bassler BL, Stone HA.** 2013. Biofilm streamers cause catastrophic disruption of flow with consequences for environmental and medical systems. Proc. Natl. Acad. Sci. U. S. A. **110:**4345–4350. http://dx.doi.org/10.1073/pnas.1303641110.
10. **Seminara A, Angelini TE, Wilking JN, Vlamakis H, Ebrahim S, Kolter R, Weitz DA, Brenner MP.** 2012. Osmotic spreading of *Bacillus subtilis* biofilms driven by an extracellular matrix. Proc. Natl. Acad. Sci. U. S. A. **109:**1116–1121. http://dx.doi.org/10.1073/pnas.1109261108.
11. **Besemer K, Singer G, Limberger R, Chlup AK, Hochedlinger G, Hödl I, Baranyi C, Battin TJ.** 2007. Biophysical controls on community succession in stream biofilms. Appl. Environ. Microbiol. **73:**4966–4974. http://dx.doi.org/10.1128/AEM.00588-07.
12. **Richards MJ, Edwards JR, Culver DH, Gaynes RP.** 2000. Nosocomial infections in combined medical-surgical intensive care units in the United States. Infect. Control Hosp. Epidemiol. **21:**510–515. http://dx.doi.org/10.1086/501795.
13. **Willner D, Haynes MR, Furlan M, Schmieder R, Lim YW, Rainey PB, Rohwer F, Conrad D.** 2012. Spatial distribution of microbial communities in the cystic fibrosis lung. ISME J. **6:**471–474. http://dx.doi.org/10.1038/ismej.2011.104.
14. **Price LB, Liu CM, Frankel YM, Melendez JH, Aziz M, Buchhagen J, Contente-Cuomo T, Engelthaler DM, Keim PS, Ravel J, Lazarus GS, Zenilman JM.** 2011. Macroscale spatial variation in chronic wound microbiota: a cross-sectional study. Wound Repair Regen. **19:**80–88. http://dx.doi.org/10.1111/j.1524-475X.2010.00628.x.
15. **Pedersen SS, Høiby N, Espersen F, Koch C.** 1992. Role of alginate in infection with mucoid *Pseudomonas aeruginosa* in cystic fibrosis. Thorax **47:**6–13. http://dx.doi.org/10.1136/thx.47.1.6.
16. **Bayer AS, Speert DP, Park S, Tu J, Witt M, Nast CC, Norman DC.** 1991. Functional role of mucoid exopolysaccharide (alginate) in antibiotic-induced and polymorphonuclear leukocyte-mediated killing of *Pseudomonas aeruginosa*. Infect. Immun. **59:**302–308.
17. **Wozniak DJ, Wyckoff TJ, Starkey M, Keyser R, Azadi P, O'Toole GA, Parsek MR.** 2003. Alginate is not a significant component of the extracellular polysaccharide matrix of PA14 and PAO1 *Pseudomonas aeruginosa* biofilms. Proc. Natl. Acad. Sci. U. S. A. **100:**7907–7912. http://dx.doi.org/10.1073/pnas.1231792100.
18. **Friedman L, Kolter R.** 2004. Two genetic loci produce distinct carbohydrate-rich structural components of the *Pseudomonas aeruginosa* biofilm matrix. J. Bacteriol. **186:**4457–4465. http://dx.doi.org/10.1128/JB.186.14.4457-4465.2004.
19. **Friedman L, Kolter R.** 2004. Genes involved in matrix formation in *Pseudomonas aeruginosa* PA14 biofilms. Mol. Microbiol. **51:**675–690. http://dx.doi.org/10.1046/j.1365-2958.2003.03877.x.
20. **Yang L, Hu Y, Liu Y, Zhang J, Ulstrup J, Molin S.** 2011. Distinct roles of extracellular polymeric substances in *Pseudomonas aeruginosa* biofilm development. Environ. Microbiol. **13:**1705–1717. http://dx.doi.org/10.1111/j.1462-2920.2011.02503.x.
21. **Colvin KM, Gordon VD, Murakami K, Borlee BR, Wozniak DJ, Wong GC, Parsek MR.** 2011. The Pel polysaccharide can serve a structural and protective role in the biofilm matrix of *Pseudomonas aeruginosa*. PLoS Pathog. **7:**e1001264. http://dx.doi.org/10.1371/journal.ppat.1001264.
22. **Ma L, Conover M, Lu HP, Parsek MR, Bayles K, Wozniak DJ.** 2009. Assembly and development of the *Pseudomonas aeruginosa* biofilm matrix. PLoS Pathog. **5:**e1000354. http://dx.doi.org/10.1371/journal.ppat.1000354.
23. **Zhao K, Tseng BS, Beckerman B, Jin F, Gibiansky ML, Harrison JJ, Luijten E, Parsek MR, Wong GC.** 2013. Psl trails guide exploration and microcolony formation in *Pseudomonas aeruginosa* biofilms. Nature **497:**388–391. http://dx.doi.org/10.1038/nature12155.
24. **Waigh TA.** 2005. Microrheology of complex fluids. Rep. Prog. Phys. **68:**685–742. http://dx.doi.org/10.1088/0034-4885/68/3/R04.
25. **Savin T, Doyle PS.** 2005. Static and dynamic errors in particle tracking microrheology. Biophys. J. **88:**623–638. http://dx.doi.org/10.1529/biophysj.104.042457.
26. **Yang YL, Lin J, Kaytanli B, Saleh OA, Valentine MT.** 2012. Direct correlation between creep compliance and deformation in entangled and sparsely crosslinked microtubule networks. Soft Matter **8:**1776–1784. http://dx.doi.org/10.1039/c2sm06745e.
27. **Langley NR, Polmanteer KE.** 1974. Relation of elastic modulus to crosslink and entanglement concentrations in rubber networks. J. Polym. Sci. Part B Polym. Physiol. **12:**1023–1034. http://dx.doi.org/10.1002/pol.1974.180120601.
28. **Körstgens V, Flemming HC, Wingender J, Borchard W.** 2001. Influence of calcium ions on the mechanical properties of a model biofilm of mucoid *Pseudomonas aeruginosa*. Water Sci. Technol. **43:**49–57.
29. **Seviour T, Malde AK, Kjelleberg S, Yuan Z, Mark AE.** 2012. Molecular dynamics unlocks atomic level self-assembly of the exopolysaccharide matrix of water-treatment granular biofilms. Biomacromolecules **13:**1965–1972. http://dx.doi.org/10.1021/bm3005808.
30. **Kundukad B, van der Maarel JR.** 2010. Control of the flow properties of DNA by topoisomerase II and its targeting inhibitor. Biophys. J. **99:**1906–1915. http://dx.doi.org/10.1016/j.bpj.2010.07.013.
31. **Rogers SS, van der Walle C, Waigh TA.** 2008. Microrheology of bacterial biofilms in vitro: *Staphylococcus aureus* and *Pseudomonas aeruginosa*. Langmuir **24:**13549–13555. http://dx.doi.org/10.1021/la802442d.
32. **Galy O, Latour-Lambert P, Zrelli K, Ghigo JM, Beloin C, Henry N.** 2012. Mapping of bacterial biofilm local mechanics by magnetic microparticle actuation. Biophys. J. **103:**1400–1408. http://dx.doi.org/10.1016/j.bpj.2012.07.001.
33. **Yang L, Hengzhuang W, Wu H, Damkiaer S, Jochumsen N, Song Z, Givskov M, Høiby N, Molin S.** 2012. Polysaccharides serve as scaffold of biofilms formed by mucoid *Pseudomonas aeruginosa*. FEMS Immunol. Med. Microbiol. **65:**366–376. http://dx.doi.org/10.1111/j.1574-695X.2012.00936.x.
34. **Colvin KM, Irie Y, Tart CS, Urbano R, Whitney JC, Ryder C, Howell PL, Wozniak DJ, Parsek MR.** 2012. The Pel and Psl polysaccharides provide *Pseudomonas aeruginosa* structural redundancy within the biofilm matrix. Environ. Microbiol. **14:**1913–1928. http://dx.doi.org/10.1111/j.1462-2920.2011.02657.x.
35. **Ciofu O, Lee B, Johannesson M, Hermansen NO, Meyer P, Høiby N, Scandinavian Cystic Fibrosis Study Consortium.** 2008. Investigation of the *algT* operon sequence in mucoid and non-mucoid *Pseudomonas aeruginosa* isolates from 115 Scandinavian patients with cystic fibrosis and in 88 in vitro non-mucoid revertants. Microbiology **154:**103–113. http://dx.doi.org/10.1099/mic.0.2007/010421-0.
36. **Klausen M, Aaes-Jørgensen A, Molin S, Tolker-Nielsen T.** 2003. Involvement of bacterial migration in the development of complex multicellular structures in *Pseudomonas aeruginosa* biofilms. Mol. Microbiol. **50:**61–68. http://dx.doi.org/10.1046/j.1365-2958.2003.03677.x.
37. **Allesen-Holm M, Barken KB, Yang L, Klausen M, Webb JS, Kjelleberg S, Molin S, Givskov M, Tolker-Nielsen T.** 2006. A characterization of DNA release in *Pseudomonas aeruginosa* cultures and biofilms. Mol. Microbiol. **59:**1114–1128. http://dx.doi.org/10.1111/j.1365-2958.2005.05008.x.
38. **Sakuragi Y, Kolter R.** 2007. Quorum-sensing regulation of the biofilm matrix genes (*pel*) of *Pseudomonas aeruginosa*. J. Bacteriol. **189:**5383–5386. http://dx.doi.org/10.1128/JB.00137-07.
39. **Joyce JG, Abeygunawardana C, Xu QW, Cook JC, Hepler R, Przysiecki CT, Grimm KM, Roper K, Ip CC, Cope L, Montgomery D, Chang M, Campie S, Brown M, McNeely TB, Zorman J, Maira-Litrán T, Pier GB, Keller PM, Jansen KU, Mark GE.** 2003. Isolation, structural character-

ization, and immunological evaluation of a high-molecular-weight exopolysaccharide from *Staphylococcus aureus*. Carbohydr. Res. **338:** 903–922. http://dx.doi.org/10.1016/S0008-6215(03)00045-4.

40. **Wang S, Parsek MR, Wozniak DJ, Ma LZ.** 2013. A spider web strategy of type IV pili-mediated migration to build a fibre-like Psl polysaccharide matrix in *Pseudomonas aeruginosa* biofilms. Environ. Microbiol. **15:** 2238–2253. http://dx.doi.org/10.1111/1462-2920.12095.
41. **Cooley BJ, Thatcher TW, Hashmi SM, L'Her G, Le HH, Hurwitz DA, Provenzano D, Touhami A, Gordon VD.** 2013. The extracellular polysaccharide Pel makes the attachment of *Pseudomonas aeruginosa* to surfaces symmetric and short-ranged. Soft Matter **9:**3871–3876. http://dx.doi.org/10.1039/c3sm27638d.
42. **Koch B, Jensen LE, Nybroe O.** 2001. A panel of Tn7-based vectors for insertion of the *gfp* marker gene or for delivery of cloned DNA into Gram-negative bacteria at a neutral chromosomal site. J. Microbiol. Methods **45:**187–195. http://dx.doi.org/10.1016/S0167-7012(01)00246-9.
43. **Yang L, Liu Y, Markussen T, Høiby N, Tolker-Nielsen T, Molin S.** 2011. Pattern differentiation in co-culture biofilms formed by *Staphylococcus aureus* and *Pseudomonas aeruginosa*. FEMS Immunol. Med. Microbiol. **62:**339–347. http://dx.doi.org/10.1111/j.1574-695X.2011.00820.x.
44. **Tolker-Nielsen T, Sternberg C.** 2005. Growing and analyzing biofilms in flow chambers. Curr. Protoc. Microbiol. **Chapter 1:**Unit 1B.2. http://dx.doi.org/10.1002/9780471729259.mc01b02s21.
45. **Kim YS, Kundukad B, Allahverdi A, Nordenskold L, Doyle PS, van der Maarel JRC.** 2013. Gelation of the genome by topoisomerase II targeting anticancer agents. Soft Matter **9:**1656–1663. http://dx.doi.org/10.1039/c2sm27229f.